JTTEE5 10:611-617

Mo_5Si_3-B and $MoSi_2$ Deposits Fabricated by Radio Frequency Induction Plasma Spraying

X. Fan and T. Ishigaki

(Submitted 16 May 2000; in revised form 24 October 2000)

Induction plasma-spray processing was used to produce free-standing parts of Mo_5Si_3-B composite and $MoSi_2$ materials. The oxidation resistance, up to 1210 °C, of the Mo_5Si_3-B composite was compared with $MoSi_2$, which is known to be resistant to high-temperature oxidation. The deposits were oxidized isothermally in air at atmospheric pressure. The structural performance of these materials under high-temperature oxidation conditions was found to depend on the boron content in the specimens. In particular, the composite containing 2 wt.% boron exhibited excellent resistance to oxidation, as indicated by the specimen mass change, which was found to be near zero after the 24 h oxidation test.

Keywords boron-Mo_5Si_3 composite, induction plasma spraying, $MoSi_2$, oxidation resistance

1. Introduction

Materials based on molybdenum disilicide ($MoSi_2$) have been under active development over recent decades because of their potential to function well in high-temperature environments.[1] A major obstacle impeding the attainment of full satisfaction for $MoSi_2$ performance in high-temperature structural applications is its questionable mechanical properties. High rates of creep at temperatures above 1200 °C make the application of $MoSi_2$ difficult where a reliable, high-temperature structural material is required. On the other hand, the low silicon-content silicide, Mo_5Si_3, possesses high creep resistance, which is comparable to the current generation of nickel-based, single crystal superalloys.[2–4] A creep rate for Mo_5Si_3 of 4×10^{-8} s^{-1} was measured at 69 MPa and 1200 °C, this value being nearly 5 times lower than that for $MoSi_2$ under the same conditions (2.1×10^{-7} s^{-1}).[4] However, the high-temperature oxidation resistance of Mo_5Si_3 is very poor, and this is the main reason that this silicide has long been ignored for high-temperature structural applications. If the oxidation resistance of the Mo_5Si_3 phase could be improved, while retaining its excellent creep resistance, this material would show strong promise as a candidate for such high-temperature structural applications.

The oxidation behavior of Mo_5Si_3 specimens is characterized by the formation of a porous surface scale and the oxidative loss of molybdenum (as MoO_3) at temperatures below about 1650 °C, with transformation to a protective scale and passivating oxidation at higher temperatures.[5] Some experimental data[6,7] has indicated that during Mo_5Si_3 oxidation at temperatures below 1650 °C, the oxidation interface becomes silicon-depleted because the silicon consumption rate exceeds the maximum rate of the silicon supply. Therefore, the scale ruptures and becomes nonpassivating. The mechanism proposed for the higher temperature passivation is that of temperature-dependent lateral flow of amorphous SiO_2 to form a continuous, oxygen excluding layer.

It has also been reported that the incorporation of small quantities of elemental boron (0.8 to 1.9 wt.%) into the Mo_5Si_3 matrix improves the high-temperature oxidation behavior of Mo_5Si_3 in the temperature range of 800 to 1300 °C, comparable to that of $MoSi_2$.[8,9] The oxidation rate for Mo_5Si_3 was decreased by 5 orders of magnitude at 1200 °C and the "pest" oxidation of Mo_5Si_3 at 800 °C was also eliminated by "doping" with less than 2 wt.% boron. The mechanism for the improved oxidation resistance of boron-doped Mo_5Si_3 is believed to lie in the formation of a low-viscosity borosilicate glass that closes the pores formed by volatilization of MoO_3 during the initial transient-oxidation period and, subsequently, forms a coherent scale over the test specimen.[10]

Until now, the previously reported boron-modified Mo_5Si_3 materials have been prepared mainly by sintering or hot isostatic pressing (HIP) of powders.[8–10] However, plasma-spray processing has recently been demonstrated to be a viable technique also for the production of dense, monolithic, and composite forms.[11] In other applications, this process has evolved to provide greater flexibility for the fabrication of shapes and to reduce the number of process steps compared to that required in conventional methods. For intermetallics, plasma-spray technology provides further advantages; *e.g.*, the combined high temperatures and rapid solidification rates have reduced segregation and residual stresses in intermetallics that typically limit the "formability" of such brittle materials, as well as improving the ductility and tensile strength of fabricated shapes.

In the present investigation, induction plasma-spray processing was used to produce free-standing parts of Mo_5Si_3-B composition, the boron and Mo_5Si_3 powders being blended to form the initial spray powders. The Mo_5Si_3-B composites were prepared in order to study the effects of the boron additions and the relationship between boron content and product material performance. The oxidation resistance for each of these composites was compared to those of Mo_5Si_3 and $MoSi_2$ plasma-spray deposits, produced under identical conditions.

Takamasa Ishigaki, National Institute for Materials Science, Advanced Materials Laboratory, 1-1, Namiki, Tsukuba-shi, Ibaraki 305-0044, Japan; and **Xiaobao Fan,** TEKNA Plasma Systems, Inc., Sherbrooke, QC J1L 1X7, Canada. Contact e-mail: ishigaki.takamasa@nims.go.jp.

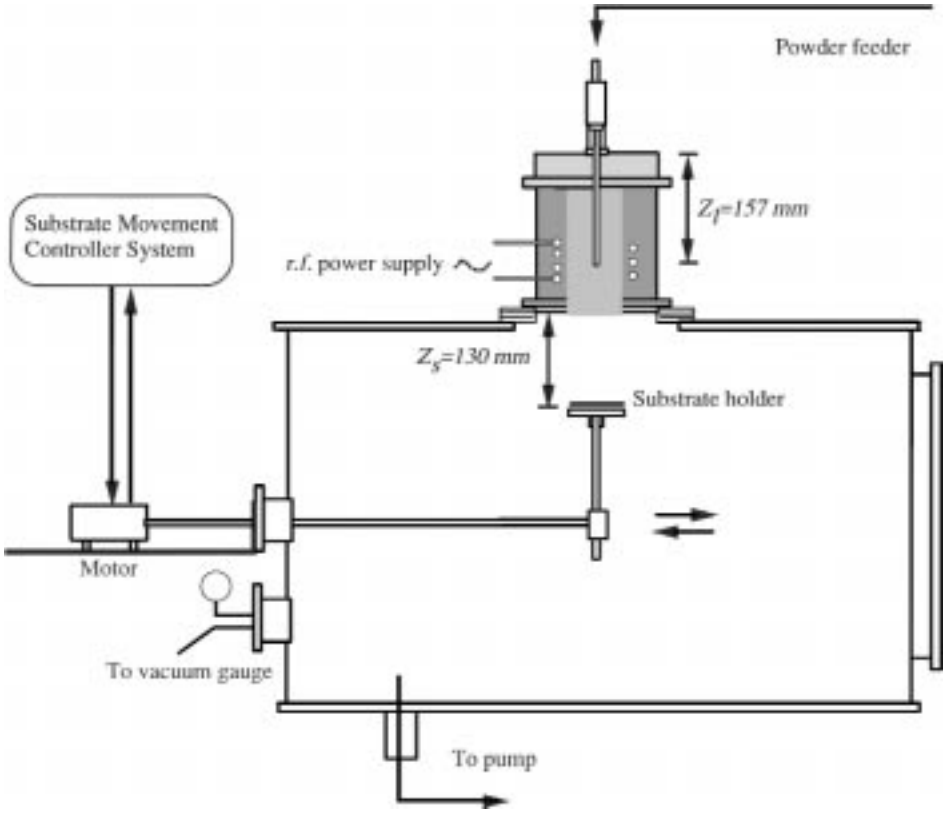

Fig. 1 The schematic view of the induction plasma-spraying installation

2. Experimental Procedure

2.1 Induction Plasma Spraying Apparatus

The complete experimental apparatus employed for this work consisted of an induction plasma torch and matching radio-frequency power supply equipment, a hermetically sealed cylindrical spray chamber, and a powder feeding system. The induction plasma torch (Model PL-50, TEKNA Plasma Systems. Inc., Sherbrooke, QC, Canada) used a water-cooled ceramic-plasma confinement tube incorporating a 3-turn induction coil; as illustrated in Fig. 1. The coil was connected to the radio-frequency power supply (2 MHz, Nihon Koshuha Co., Ltd., Yokohama, Japan) through the tank circuit.

The cylindrical spray chamber (80 cm internal diameter and 100 cm height) was made as a water-cooled stainless steel structure. The induction plasma torch was fixed at the center of the upper port of the chamber *via* the bolted flange. An inspection window on the front port and another two at positions in the side the chamber (not shown in the schema of Fig. 1) permitted visual supervision of the deposition procedure. Oil-filled rotary pumps were interfaced at the bottom of the spray chamber to maintain the necessary condition of reduced pressure. The static low pressure in the spray chamber was maintained below 1 torr by the pumping system (1 torr equals 0.133 kPa). Exhaust gases extracted from the chamber were initially passed through a filter to collect particles carried off by the gas stream before the latter entered the extraction line for further wet scrubbing treatment and eventual discharge to the atmosphere.

A water-cooled stainless steel probe, axially penetrating the torch head, injected the reactant powders into the plasma. The position of the probe was adjusted to place its tip at the center plane of the induction coil (Fig. 1).

2.2 Spraying Procedure

The powder blends were prepared by mechanical mixing of Mo_5Si_3 powders (Nihon New Metals, Inc., Toyonaka, Osaka, Japan) and boron powders (Cerac, Inc., Milwaukee, WI) in certain mass ratios in a ball-milling jar for 24 h. The screen size gradation of the Mo_5Si_3 particles was $-38 + 20$ μm, while the average particle diameter of the boron powders was 0.19 μm. The assayed chemical composition of the Mo_5Si_3 particles was Si-14.52, C-0.01, O-0.28, and Fe-0.04 (wt.%). The Mo_5Si_3 powder proved to be of very pure phase and close to stoichiometric composition (theoretical Si wt.% in the compound Mo_5Si_3 is 14.95 wt.%). The x-ray diffractometry (XRD) pattern of the Mo_5Si_3 powder corresponded well with that of the JCPDS card 34-0371 for Mo_5Si_3. The purity of the initial boron powder was claimed to be >9.9+%, with Ca and Mg content each at less than 0.001%. The boron powder was amorphous; the only XRD peak for a crystalline phase belongs to the oxide, B_2O_3, indicating that some oxygen uptake had occurred during boron powder production. Molybdenum disilicide powder was also supplied by Japan New Metals, Inc. The screen size gradation was $-38 + 20$ μm. These powders contain tetragonal phase α-$MoSi_2$ exclusively, along with traces of free residual silicon. The assayed chemical composition was Si-36.83, C-0.02, O-0.26, and Fe-

0.09 (wt.%), where the powder has little deviation from stoichiometry. The theoretical Si wt.% in the compound $MoSi_2$ is 36.93 wt.%.

The premixed powders were fed to the torch by means of a Hi-T Drive Servo actuator powder feeder (Plasma Giken Co., Ltd., Toda, Saitama, Japan) in which powders are agitated by mechanical stirring and then conveyed by the drive disk to the metering orifice. The process-carrier gas transports the powder through a narrow pipeline to the torch injector probe. The mean powder feed rate was determined mainly by the rotation speed of the drive disk. Thus, at 3 rpm and 5 L/min Ar carrier gas flow, the powder delivery rate was 1.6 to 1.7 cm^3/min, corresponding to ~14 g/min (standard deviation $\sigma = 0.4$) for Mo_5Si_3 and other Mo_5Si_3-B blending powders, and ~10 g/min ($\sigma = 0.2$) for $MoSi_2$ powder.

In the spray chamber, a reciprocating substrate-translation system activated by a programmable electric-drive mechanism provided traversing deposition motion. The length of each pass and the velocity of the traverse were both continuously adjustable, the spray distance being varied by simply changing the fixing position of the substrate support rod in the fixture. The deposits were prepared by spraying plasma-melted powders onto 100 mm diameter steel substrates, pretreated with BN releaser to provide a single surface layer of BN, facilitating deposit separation from the substrate as a free-standing part.

The induction plasma-spraying parameters employed in this work are summarized in Table 1. The inductive power level was fixed at 25 kW, though the TEKNA PL-50 torch can be operated up to 60 kW. The employment of a relatively low plasma-power level was aimed at suppressing molybdenum silicide decomposition by the high-temperature plasma.[12] The spray distance, Z_S, was set at 130 mm, having been determined during several runs of preliminary experiments. It is a compromise between two conflicting circumstances. (1) At relatively close spraying distances, droplets retain their molten state at the time of impact on the substrate so that dense coatings and high deposition efficiencies can be achieved. (2) The risk of melting the substrate material must be avoided, and the refusion of the deposit is equally undesirable.

Because of capacity limitations in the chamber pumping system, the spray processing in this investigation was not performed at constant pressure. A relatively low pressure was desired to give the particles higher substrate-impingement momentum and to retain lower melt particle-surface temperature (the plasma residence time for particles was short at the lower pressure condition) to avoid decomposition. Unfortunately, the fine particles resulting from material vaporization in the course of spraying tended to block the filter, making the maintenance of low pressure difficult and raising the pressure in the spray chamber. Typically, spraying began at 200 torr and ended at 400 torr, an operation occupying about 6 min. With the substrate "pass" length of 10 mm, sprayed deposits took on the appearance of conical hills but with flat tops, the heights of the deposits ranging from 10 to 13 mm. Deposition efficiencies (the ratio of the mass of spray deposit to the mass of the material sprayed) of about 84% were achieved.

2.3 Characterization of Deposits

After plasma spray preparation, the deposits were cut into square slices of 10 × 10 × 3 mm for various tests. The porosity of the deposits was measured by mercury intrusion porosimetry (MIP) (Model AutoPore II 9220, Micrometrics Instrument Corp., Norcross, GA). Fractured specimens were examined by scanning electron microscopy (SEM) (Model ISI-DS130, Akashi Co., Tokyo) to observe their fractographs. Polished samples were examined by XRD to determine the phases present. Polished cross sections were also examined by SEM and energy dispersion spectrum to reveal the microstructure of deposits and the distribution of elemental boron in the composite. For the assessment of oxidation resistance, sliced samples were further cut into 3 × 3 × 2 mm cubes, placed in platinum crucibles (5 mm in diameter and 2.5 mm in height), and subjected to high-temperature oxidation testing in a thermogravimetric analyzer (TG-DTA) (Model TG-8120, Rigaku Co., Akishima, Tokyo).

Table 1 Summary of the experimental conditions

Plasma gas		Ar 30 L/min
Sheath gas		Ar 85 L/min + H_2 5L/min
Carrier gas		Ar 5 L/min
Induction power level		25 kW
Spraying distance		130 mm
Chamber pressure		26 to 53 kPa
Powder feed rate		14 g/min
Substrate translation:	Length	10 mm
	Velocity	21 mm/min

3. Results

3.1 Phase Content and Porosity

Figure 2 shows x-ray diffraction patterns of induction plasma-sprayed deposits of $MoSi_2$, Mo_5Si_3, and Mo_5Si_3-B composites. The sprayed $MoSi_2$ consisted of α-$MoSi_2$ and a trace of Mo_5Si_3. In the case of Mo_5Si_3 spraying, the deposit was composed of pure Mo_5Si_3. The major phase in the as-sprayed Mo_5Si_3-B 2 wt.% deposit was Mo_5Si_3; however, the molybdenum boride phase, MoB, was detected and identified by reference to JCPDS card 6-0644. The peaks of MoB are marked in Fig. 2(c); all remaining unmarked peaks represent the Mo_5Si_3 phase (Fig. 2b). The formation of MoB was due to reaction between reactant powders under the high-temperature plasma conditions.[13] MoB was also found in the as-sprayed deposits of Mo_5Si_3-B 1.5 wt.% but not in the deposits of the nominal Mo_5Si_3-B 1 wt.% and Mo_5Si_3-B 0.5 wt.% compositions. This is not surprising when the sensitivity of the XRD technique (~5 vol.%) is taken into account. The 0.5 and 1 wt.% levels of input boron are equivalent to 1.6 and 3.2 vol.% in the initial reagent powders, respectively. Therefore, even if all boron reacts with molybdenum silicide and is converted into MoB, it would still be difficult to detect this product by the XRD technique.

The porosities of the as-sprayed deposits were measured by MIP, and the results are summarized in Table 2, together with each sample's phase contents, as detected by the XRD test. Because of the relatively "cool" induction plasma-spray conditions employed in this investigation, the porosity of the deposits was a little high, on average ~9.2 %, with pore radii ranging between 0.1 and 0.7 μm and bulk densities of only 90.4% of theoretical. Nevertheless, the relatively cool spray conditions used effectively suppressed

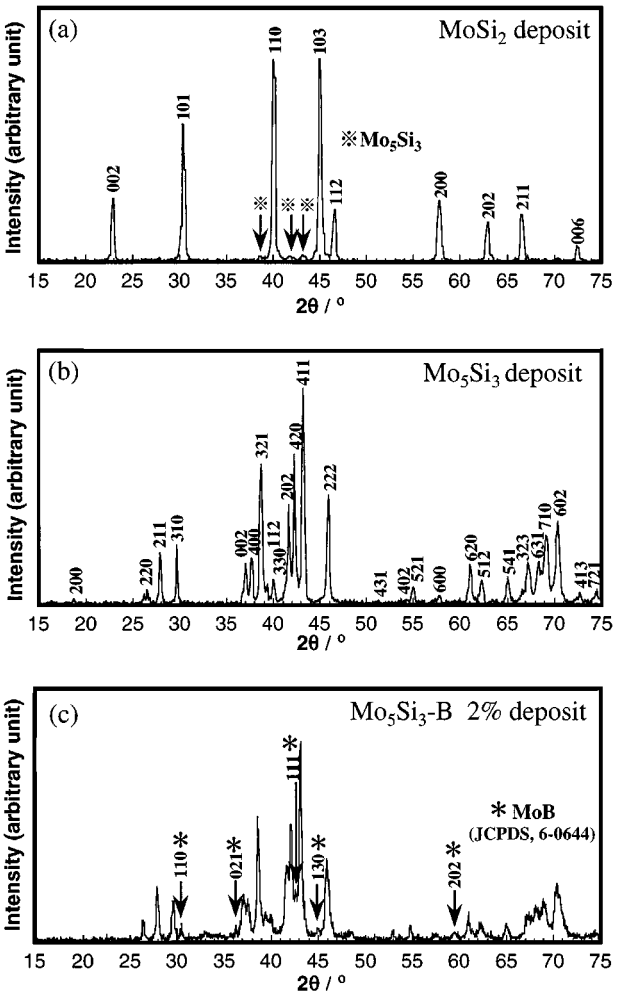

Fig. 2 The XRD patterns of deposits of (**a**) $MoSi_2$, (**b**) Mo_5Si_3, and (**c**) Mo_5Si_3-B 2 wt.%

Table 2 Porosity and phase content of Mo_5-Si_3-B composite deposits

Specimen	Nominal composition	Porosity (%)	Phase Mo_5Si_3	Content $MOSi_2$	XRD MoB
A	$MoSi_2$	10.3		√	
B	Mo_5Si_3	8.5	√		
C	0.5 wt.% B-Mo_5Si_3	9.9	√		
D	1 wt.% B-Mo_5Si_3	10.7	√		
E	1.5 wt.% B-Mo_5Si_3	8.3	√		√
F	2 wt.% B-Mo_5Si_3	7.7	√		√

the decomposition of molybdenum silicides. Deposits of $MoSi_2$ and Mo_5Si_3 materials, to be used as controls for the oxidation resistance test, were prepared using the same spray-processing parameters.

3.2 Microstructure

Figure 3 presents fractographs of Mo_5Si_3-2 wt.% B composite deposits. As the production of deposits or coatings of various materials by plasma spraying process is essentially a "piling up" of particles on the substrate, the splats, formed by melt particles impacting and solidifying on the substrate, are the fundamental units in the structure of deposits or coatings. The fracture morphology shown in Fig. 3(a) represents a fracture surface parallel to the substrate surface, the rupture occurred mainly between splats, leaving a smooth fracture surface. This is a prominent characteristic of plasma-sprayed deposits and coating microstructures, according to McPherson,[14] where there is limited real contact between the rapidly solidifying particles, the actual area of contact has been estimated at only around 20%. Therefore, the fracture was likely to be effected by "shearing" those weak "joints" between splats. However, the fractograph along the deposit building direction (normal to the substrate surface) displays a trans-splat morphology because splats formed in the induction plasma-spray process usually possess a relatively high ratio of their thickness with respect to their span.[15] The stress applied along the normal direction has to "break" individual splats so that the crack front forms and propagates to create the fracture surface. The laminate microstructure of the as-sprayed deposit is, thus, clearly seen in Fig. 3(b).

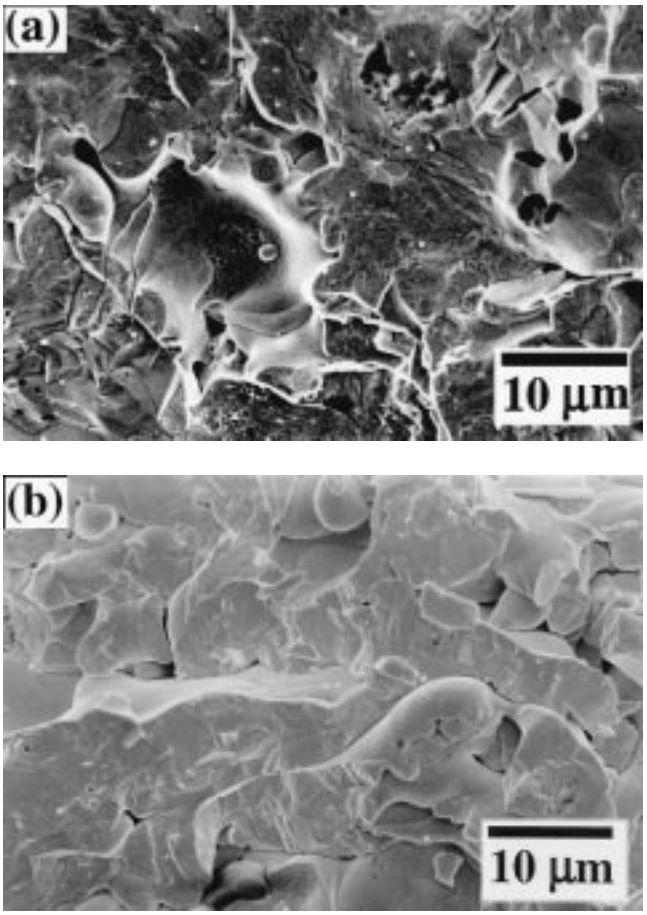

Fig. 3 Fractographs of the Mo_5Si_3-B 2 wt.% composite deposits (**a**) parallel to the substrate surface and (**b**) normal to the substrate surface

The polished cross section was subjected to SEM examination. The EDS spectrum was taken on a dark round part. The boron K_α peak (0.18 keV) is recognized in the EDS result in Fig.

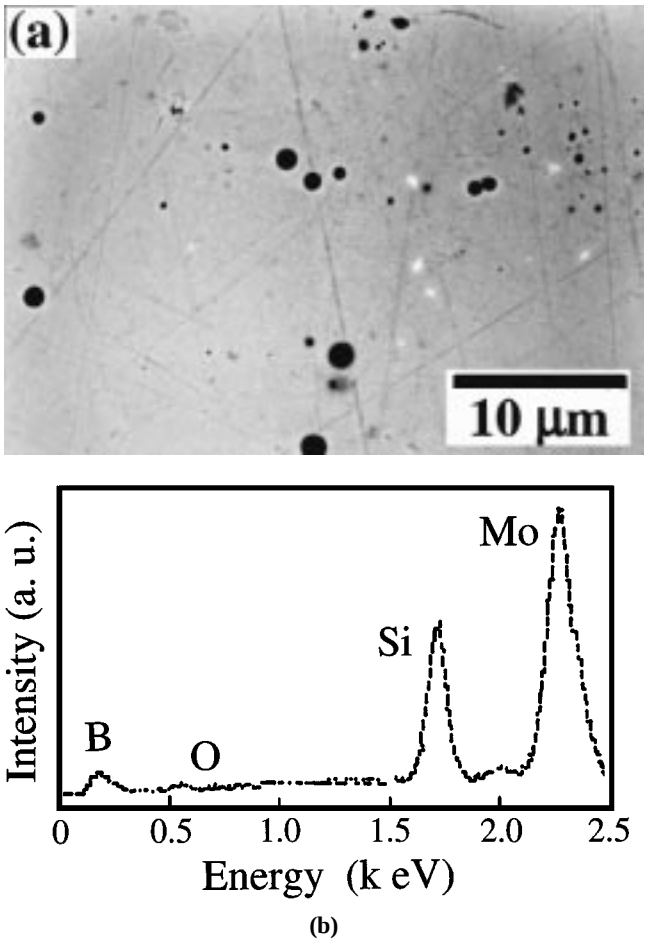

Fig. 4 The cross section of the sample of Mo_5Si_3-B 2 wt.%: (**a**) boron spheres in the Mo_5Si_3 matrix and (**b**) the EDS on a dark round part shown in (**a**)

4(b), although the signal also includes one from the electron-penetrated area. It is seen that the boron phase predominately takes the spherical form inside the Mo_5Si_3 matrix (Fig. 4a). The dimensions of these spheres range from 0.1 to 5 μm. Despite the fact that input boron powders had been well dispersed and mechanically stuck to the surfaces of coarse Mo_5Si_3 powders during the prespray blending, the microstructure revealed in Fig. 4(a) indicates that coagulation of the boron occurred when the blended powders passed through the high-temperature plasma. This suggests that there was a lack of good wetting behavior between molten boron and molybdenum silicide materials, resulting from their physical properties. Agglomerated boron spheres, formed during the spray process, could also be observed on the deposit surfaces.

3.3 High-Temperature Oxidation Resistance

Oxidation resistance of the specimens was evaluated through the TG tests. After mounting the specimen-loaded crucible in the TG instrument, the specimen temperature was then increased at 20 °C/min to the preset temperature, 1210 °C, and held for 24 h, during which time the mass changes and temperature of the specimens were continuously recorded. Figure 5 shows plots of

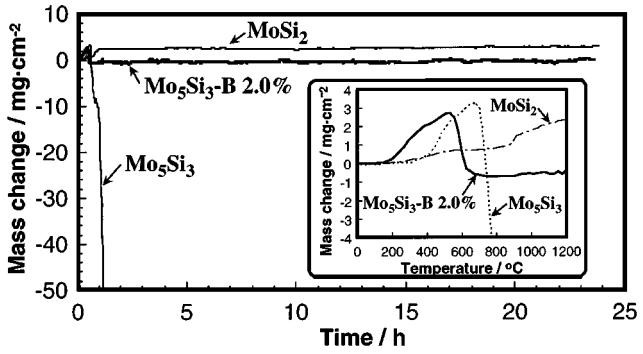

Fig. 5 Mass change of $MoSi_2$, Mo_5Si_3, and Mo_5Si_3-B specimens as a function of time on oxidation in air at 1210 °C. Plots include initial heating at 20 °C/min, and the transition behavior of mass change is shown as an inset small figure

the mass changes versus time for the induction plasma-sprayed deposits of $MoSi_2$, Mo_5Si_3, and Mo_5Si_3-2 wt.% B composites in oxidation at 1210 °C in air. These plots include the initial "ramping up" of temperature at 20 °C/min. During the initial stage of these tests, all specimens (except $MoSi_2$) demonstrated rapid mass gain up to a certain value, which was then followed by a drastic mass loss. This initial transient behavior of the specimens is displayed in a small inset figure.

It could also be observed with the unaided eye that the Mo_5Si_3 specimen had become a chalky white mass after 24 h of oxidation at 1210 °C, while only small quantities of such white products had been seen in the Mo_5Si_3-B composites with boron content of 0.5 and 1 wt.%. For composite deposits with boron content greater than 1 wt.%, the surface of the specimens after oxidation exhibited a dark blue color. The $MoSi_2$ specimen appeared to keep the same luster as was evident prior to the oxidation.

4. Discussion

As far as the authors' present knowledge goes, no report has been made on the preparation of Mo_5Si_3-B composite materials *via* the plasma-spray route. The primary motivation of the present investigation has been the validation of the induction plasma-spray process for the preparation of free-standing parts of Mo_5Si_3-B composite materials; the investigation of the oxidation mechanism will be the subject of a further study. Here, a brief description only is given of the Mo_5Si_3-B composite material performance under high-temperature oxidation conditions.

4.1 Improvement of Oxidation Resistance of Mo_5Si_3 by Boron Addition

The oxidation behavior of Mo_5Si_3 at elevated temperatures can be described as catastrophic. In fact, it was observed during this investigation, that the mass loss sustained by the Mo_5Si_3 specimen was 169 m/cm^2 (equivalent to 70% material loss) in 2.2 h. After this period, no further specimen weight loss was observed up to the end of the oxidation test (not shown in Fig. 5). On the basis of the mass loss and morphology of the post oxidation specimen, it is believed that the Mo_5Si_3 had been totally converted to the cristobalite form of silica. This phenomena has

been also reported in previous studies.[6,9] The oxidation rate of the Mo_5Si_3 specimen, after an initial transient period, can be considered as linear and approximately equal to $-7.2 \times 10^{+1}$ mg/cm^2 · h. Meyer *et al.*[9] have reported the average linear rate constant for their powder processed Mo_5Si_3 specimens at 1200 °C (for a 3 h run in a flow of compressed breathing air at 100 mL/min) as high as $-1.3 \times 10^{+3}$ mg/cm^2 · h. Their test specimen was a pellet of sintered Mo_5Si_3 powder; the bulk density of which was reported to be 99% of theoretical.

The addition of boron to Mo_5Si_3 provides a clear improvement in oxidation resistance. The specimens with boron contents of 1.5 and 2 wt.% demonstrated very encouraging results: the mass change of the Mo_5Si_3-B 1.5 wt.% composite was <1%, while for the Mo_5Si_3-B 2 wt.%, the mass change was near zero. In fact, after an initial transient period, the mass change of this specimen was slightly variable but did not exceed the range (-0.97, $+0.31$) mg/cm^2, and the mass of the specimen was essentially the same at the end of the 24 h oxidation as that prior to the test. The $MoSi_2$ deposit, prepared under the same induction plasma-spraying condition, was employed here as a reference; its oxidation behavior exhibiting a mass gain feature amounting to a 2% mass increment following high-temperature oxidation.

4.2 Oxidation Behavior of Mo_5Si_3 and $MoSi_2$

There have been many publications[4–7,16–24] on the topic of $MoSi_2$ oxidation behavior, in addition to the low silicides of Mo_5Si_3 and Mo_3Si. In fact, the outstanding oxidation resistance of $MoSi_2$, ascribed to the formation of a self-healing, high silica-content glass coating, has been an important factor impelling research and development activities on high-temperature structural applications over several decades. On the other hand, no fully protective layer forms on a specimen of Mo_5Si_3 at an oxygen pressure of 1 atm over the temperature range, 484 to 1600 °C.[6] Large mass losses are characteristic of the oxidation behavior of Mo_5Si_3 materials.

The widely accepted oxidation mechanism for $MoSi_2$ is briefly summarized as

$$5MoSi_2 + 7O_2 \rightarrow Mo_5Si_3 + 7SiO_2 \quad \text{(Eq 1)}$$

Further, many people prefer to consider the oxidation product at the right-hand side of reaction 1 as a ternary Mo-Si-O glass.[16] The thin, continuous layer of protective oxide (SiO_2), formed during oxidation, corresponds to the small mass gain of $MoSi_2$ materials. For Mo_5Si_3 materials, however,[9] there are three possible competing net reactions taking place during the course of the oxidation:

$$2Mo_5Si_3 + 21O_2 \rightarrow 10MoO_3(\uparrow) + 6SiO_2 \quad \text{(Eq 2)}$$

$$3Mo_5Si_3 + 4O_2 \rightarrow 5Mo_3Si + 4SiO_2 \quad \text{(Eq 3)}$$

$$Mo_5Si_3 + 3O_2 \rightarrow 5Mo + 3SiO_2 \quad \text{(Eq 4)}$$

The volatilization of MoO_3 formed in reaction 2 accounts for the mass loss sustained by Mo_5Si_3 materials; while the formation of SiO_2 in reactions 3 and 4 results in the oxidation mass gain.

Meyer *et al.*[9] have described the transient behavior of Mo_5Si_3 specimens in the initial oxidation stages. Therefore, a rapid mass gain occurs first, due to the formation of molybdenum oxide and SiO_2 on the silicide surface. As the oxidation temperature rises above 750 °C, a rapid mass loss occurs, indicating the presence of molybdenum oxide volatilization. This behavior of a Mo_5Si_3 specimen was also observed in the present investigation, as illustrated in the small inset figure of Fig. 5. According to the Scientific Group Thermodata Europe (GTT mbH, Herzogenrath, Germany) thermochemical databases, the equilibrium species in the vapor phase with MoO_3 solid phase are $(MoO_3)_4$, $(MoO_3)_3$, $(MoO_3)_5$, and $(MoO_3)_2$.

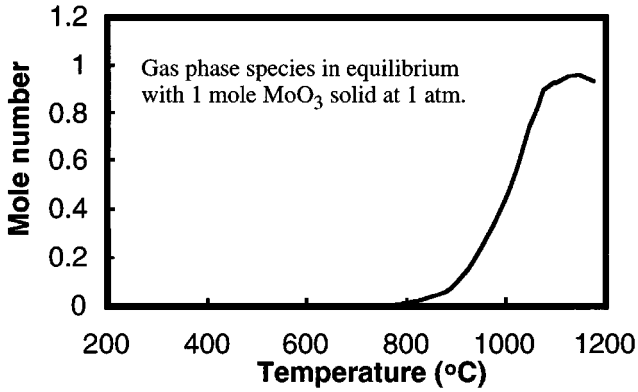

Fig. 6 Amount of the vapor species in equilibrium with 1 mole MoO_3 solid

Simple calculation suggests that the sublimation of MoO_3 solid phase becomes significant once the temperature is greater than 700 °C. (Simple thermodynamic calculations can be performed *via* the Internet where free software is available. Our estimation of the equilibrium vapor phase of MoO_3 is accomplished by the program EQUILIB-Web at the website ⟨http://www.crct.polymtl.ca/fact/websites.htm⟩ provided by the Centre for Research in Computational Thermochemistry (CRCT), Université de Montréal, Canada.) The equilibrium quantities (sum of mole numbers) of these vapor species versus temperature are shown in Fig. 6. This reasonably explains the transient behavior of Mo_5Si_3 materials in the initial temperature-rising stage.

The early oxidation behavior of a Mo_5Si_3-B composite in the transient temperature region is similar to that of undoped Mo_5Si_3, *i.e.*, an initial mass gain, followed by a mass loss. The inflection points in the mass-change plots were found to lie over a wide temperature range (from 500 to 700 °C). It is still not clear whether this shift in the inflection point has any relation to the boron content of the specimen. The Mo_5Si_3-B composite mass loss is also due to sublimation of MoO_3, as discussed previoiusly for the Mo_5Si_3 material. However, the loss as volatile B_2O_3 must also be taken into account. Meyer *et al.*[9] have mentioned this possibility for Mo_5Si_3-B composites involved in long-time oxidation tests.

The influence of the boron addition on the oxidation resistance of Mo_5Si_3 material is obvious, as is clearly demonstrated in Fig. 5. However, the composition modification seems insufficient for effective improvement of material performance if the composite boron content is less than 1 wt.%. The occurrence of such a "lower limit" to the useful boron content has also been noted for Mo_5Si_3-B composites, prepared by powder processing, this being somewhere between 0.14 and 0.91 wt.%.[9]

4.3 Advantages of Induction Plasma Spraying

It is appropriate to mention here the advantages of induction plasma processing for the preparation of molybdenum silicides and other intermetallic materials. Previous research work on the carburization[25] and nitridation[26] reactions of $MoSi_2$ powders has shown the benefits of the induction plasma process for the production of *in situ* composite powders. In the present investigation of Mo_5Si_3-B composites, the high productivity of the induction plasma-spray process may be recommended. Compared to other technologies, including sintering or HIP of powders, the preparation of Mo_5Si_3-B composites by the plasma-spray route is essentially a "one step" operation and may be implemented over a short time period. In this investigation, 6 to 7 min of spraying at a powder feed rate of 14 g/min could produce about 10 cm^3 bulk sample of Mo_5Si_3-B composite material. This powder feed rate may be readily increased to obtain larger outputs. For example, Fan *et al.*[27] have accomplished a powder feed rate of 4.2 kg/h of alumina at 40 kW, producing a deposit with less than 10% porosity. The induction plasma-spray process is, therefore, a promising method for the mass production of composite materials of this kind.

5. Conclusions

Mo_5Si_3-B composite and $MoSi_2$ materials prepared by induction plasma-spray processing were oxidized isothermally at 1210 °C in air. The material performance of Mo_5Si_3-B composites at high temperature was found to depend strongly on the composite boron content, *e.g.*, at boron contents greater than 1 wt.%; composites demonstrate encouraging oxidation resistance in the high-temperature environment. In particular, the Mo_5Si_3-B composite containing 2 wt.% boron exhibits excellent oxidation resistance, being comparable to $MoSi_2$, *e.g.*, an almost zero mass change for this material was measured after the 24 h oxidation test period.

References

1. A.K. Vasudévan and J.J. Petrovic: *Mater. Sci. Eng. A,* 1992, vol. 155, pp. 1-17.
2. D.M. Shah, D. Berczik, D.L. Anton, and R. Hecht: *Mater. Sci. Eng. A,* 1992, vol. 155, pp. 45-57.
3. M.K. Meyer, M.J. Kramer, and M. Akinc: *Intermetallics,* 1996, vol. 4, pp. 273-81.
4. D.L. Anton and D.M. Shah: *Mater. Res. Soc. Symp. Proc.,* 1991, vol. 213, pp. 733-39.
5. E. Fitzer: in *Ceramic Transactions,* vol. 10, *Corrosive and Erosive Degradation of Ceramics,* R.B. Tressler and M. McNallan, eds., American Ceramic Society, Westerville, OH, 1989, pp. 19-41.
6. R.W. Bartlett, J.W. McCamont, and P.R. Gage: *J. Am. Ceram. Soc.*, 1965, vol. 48 (11), pp. 551-58.
7. J.B. Berkowitz-Mattuck and R.R. Dils: *J. Electrochem. Soc.,* 1965, vol. 112 (6), pp. 583-89.
8. A.J. Tom, M.K. Meyer, M. Akinc, and Y. Kim: in *Processing and Fabrication of Advanced Materials for High Temperature Applications—III,* T.S. Srivatsan and V.A. Ravi, eds., TMS, Warrendale, PA, 1993, p. 413.
9. M.K. Meyer and M. Akinc: *J. Am. Ceram. Soc.,* 1996, vol. 79 (4), pp. 938-44.
10. M.K. Meyer and M. Akinc: *J. Am. Ceram. Soc.,* 1996, vol. 79 (10), pp. 2763-66.
11. R.W. Smith and R. Knight: *JOM,* 1995, vol. 8, pp. 32-39.
12. X. Fan, T. Ishigaki, and Y. Sato: *J. Mater. Res.,* 1997, vol. 12 (5), pp. 1315-26.
13. X. Fan, K. Hack, and T. Ishigaki: *Mater. Sci. Eng. A,* 2000, vol. 278($^1/_2$) pp. 46–53.
14. R. McPherson: *Surf. Coating Technol.,* 1989, vol. 39–40 (1–3), pp. 173-81.
15. X. Fan, F. Gitzhofer, and M. Boulos: *J. Thermal Spray Technol.,* 1998, vol. 7 (2), pp. 197-204.
16. A.W. Searcy: *J. Am. Ceram. Soc.,* 1957, vol. 40 (12), pp. 431-35.
17. G.B. Cherniak and G. Elliot: *J. Am. Ceram. Soc.,* 1964, vol. 47 (12), pp. 136-41.
18. G.R. Blair, H. Levin, and R.E. O'Brien: *J. Am. Ceram. Soc.,* 1965, vol. 48 (8), pp. 430-32.
19. R. Beyers: *J. Appl. Phys.,* 1984, vol. 56 (1), pp. 147-52.
20. D.A. Berztiss, R.R. Cerchiara, E.A. Gulbransen, F.S. Pettit, and G.H. Meier: *Mater. Sci. Eng. A,* 1992, vol. 155, pp. 165-81.
21. J. Cook, A. Khan, E. Lee, and R. Mahapatra: *Mater. Sci. Eng. A,* 1992, vol. 155, pp. 183-98.
22. A. Mueller, G. Wang, R.A. Rapp, and T.A. Kircher: *Mater. Sci. Eng. A,* 1992, vol. 155, pp. 199-207.
23. T.C. Chou and T.G. Nieh: *J. Mater. Res.,* 1993, vol. 8 (7), pp. 1605-10.
24. T.C. Chou and T.G. Nieh: *J. Mater. Sci.,* 1994, vol. 29, pp. 2963-67.
25. X. Fan, T. Ishigaki, and Y. Sato: *J. Am. Ceram. Soc.,* 1999, vol. 82 (2), pp. 281-88.
26. X. Fan, T. Ishigaki, Y. Suetsugu, J. Tanaka, and Y. Sato: *J. Am. Ceram. Soc.,* 1998, vol. 81 (10), pp. 2517-26.
27. X. Fan, F. Gitzhofer, and M. Boulos: *J. Thermal Spray Technol.,* 1998, vol. 7 (2), pp. 247-53.